Rho GTP exchange factor ARHGEF11 regulates the integrity of epithelial junctions by connecting ZO-1 and RhoA-Myosin II signaling

Masahiko Itoh[a,1], Sachiko Tsukita[b], Yuji Yamazaki[b], and Hiroyuki Sugimoto[a]

[a]Department of Biochemistry, School of Medicine, Dokkyo Medical University, Tochigi 321-0293 Japan; and [b]Laboratory of Biological Science, Graduate School of Frontier Biosciences and Graduate School of Medicine, Osaka University, Osaka 565-0871, Japan

Edited* by Mina J. Bissell, E. O. Lawrence Berkeley National Laboratory, Berkeley, CA, and approved May 8, 2012 (received for review September 14, 2011)

The organization of the apical junctional complex and its association with the cytoskeleton is essential for the function of epithelial cells. However, knowledge about the signaling pathways that regulate these processes is still fragmentary. Here we found that ARHGEF11, a member of the RGS-RhoGEF family, associates with tight junctions (TJs) by binding to ZO-1, but not to the highly homologous ZO-2, in polarized epithelial cells. In the early phases of cell–cell contact, ARHGEF11 was located at primordial adherens junctions, and then its localization was altered to TJs as epithelial polarity was established, much like ZO-1. Knockdown of ARHGEF11 reduced the phosphorylation of myosin light chain, retarding the assembly of cell–cell junctions and the development of the paracellular barrier. Furthermore, the simultaneous knockdown of ARHGEF11 and ZO-2 resulted in significant impairment of TJs and of the perijunctional actomyosin ring; similar defects arise when both ZO-1 and ZO-2 are depleted. These results suggest that ARHGEF11 mediates RhoA–myosin light chain signaling pathways at cell–cell junctions, functioning in cooperation with ZO-1, to regulate the paracellular barrier and the organization of the apical junctional complex and perijunctional actomyosin ring of epithelial cells.

epithelial organization | cell adhesion

In multicellular organisms, polarized epithelial cells form sheet-like structures to protect underlying tissues and maintain the physiological environment (1, 2). Cells within epithelial sheets are connected by the intercellular apical junctional complex, which is important in defining the sheets' physiological functions and integrity (3). Tight junctions (TJs) are the most apical structures in the junctional complex; they connect adjacent cells in a narrow band just beneath the apical surface. Importantly, TJs create the primary barrier that prevents the passage of molecules and ions through the paracellular space between cells and restricts the diffusion of integral membrane proteins and lipids between the apical and basolateral surface of the cell, thus potentially contributing to the maintenance of cellular polarity (1).

Recent investigations have provided significant advances in understanding the molecular architecture and regulatory mechanisms of TJs (4). The ZO family proteins (ZO-1, ZO-2, and ZO-3), which are located just beneath the plasma membrane, act as scaffolds by interacting with various proteins to build the molecular platform for the TJs. ZO-1, for example, binds to claudins, ZO-2, and junctional adhesion molecule (JAM)-A via, respectively, its PDZ1, PDZ2, and PDZ3 domains (5). It also interacts with occludin and ZONAB, via its GU.K. and SH3 domains, respectively (Fig. 1*A*) (4). ZO-1's C-terminal half binds proteins such as actin and cortactin (6, 7). Because of these properties, ZO-1 is believed to connect TJ membrane proteins with the actin cytoskeleton.

Just below the apical pole of polarized epithelial cells, the actin and myosin cytoskeleton forms a characteristic structure, called the perijunctional actomyosin ring (PJAR), which encircles each cell. PJARs influence paracellular permeability and epithelial integrity by associating with TJs and adherens junctions (AJs) (3). Several studies have reported on the involvement of specific actin cytoskeletal regulatory proteins, such as Rho and myosin light chain (MLC) kinase, in organizing the PJARs (8–11). The depletion of ZO family proteins leads to the disorganization not only of TJs, but also of PJARs, resulting in impaired barrier function (12, 13). Thus, ZO family proteins could play crucial roles in the regulation of epithelial physiology. However, the molecular mechanisms underlying the ZO proteins' control of PJARs and TJs are still largely unknown.

In the present study, we identified ARHGEF11, a member of the regulator of G protein signaling (RGS)–RhoGEF family, as a ZO-1–binding regulator of junctional actomyosin in epithelial cells. ARHGEF11 was targeted to the TJs ZO-1–dependently. The depletion of ARHGEF11 affected the phosphorylated MLC (p-MLC) and delayed junction assembly and barrier formation. Furthermore, the simultaneous knockdown of ARHGEF11 and ZO-2 prevented proper establishment of the PJARs and TJs, a phenotype similar to that caused by the knockdown of both ZO-1 and ZO-2. These results suggest that ARHGEF11 could play crucial roles in epithelial barrier physiology by orchestrating the activities of RhoA and MLC at cell–cell junctions through its direct interaction with ZO-1.

Results

RGS-RhoGEF Family Protein ARHGEF11 Binds Directly to ZO-1. To elucidate the molecular mechanisms for the TJs' and PJARs' organization by ZO family proteins, especially ZO-1, we used yeast two-hybrid screening to identify regulatory molecules associated with ZO-1. As ZO-1 consists of more than 1,700 aa, we constructed bait plasmids encoding ZO-1 fragments. Clones containing three of these fragments, aa 181 to 503, aa 423 to 862, and aa 1520 to 1745, which exhibited low background in a control β-galactosidase assay, were mixed and used to screen prey library produced from mouse embryo cDNA. Among the positive clones, we focused on prey202, which encoded the carboxyl-terminal region of the RGS-RhoGEF family protein ARHGEF11, for further analysis (Fig. 1*A*).

We determined the ZO-1 region that bound prey202 by an in vitro binding experiment using recombinant proteins (Fig. 1*B*). GST (control), GST-ZO-1 (aa 181–503), GST-ZO-1 (aa 423–862) and GST-ZO-1 (aa 1520–1745) were incubated with or without a fusion protein of prey202 and maltose-binding protein (MBP; MBP-prey202). Coomassie brilliant blue staining of the eluted samples showed that GST-ZO-1(1520–1745) specifically pulled down MBP-prey202 (Fig. 1*B*, *Right*, arrowhead).

Author contributions: M.I. designed research; M.I. performed research; M.I., S.T., Y.Y., and H.S. contributed new reagents/analytic tools; M.I., S.T., and H.S. analyzed data; and M.I. wrote the paper.

The authors declare no conflict of interest.

*This Direct Submission article had a prearranged editor.

[1]To whom correspondence should be addressed. E-mail: mitoh@dokkyomed.ac.jp.

This article contains supporting information online at www.pnas.org/lookup/suppl/doi:10.1073/pnas.1115063109/-/DCSupplemental.

CELL BIOLOGY

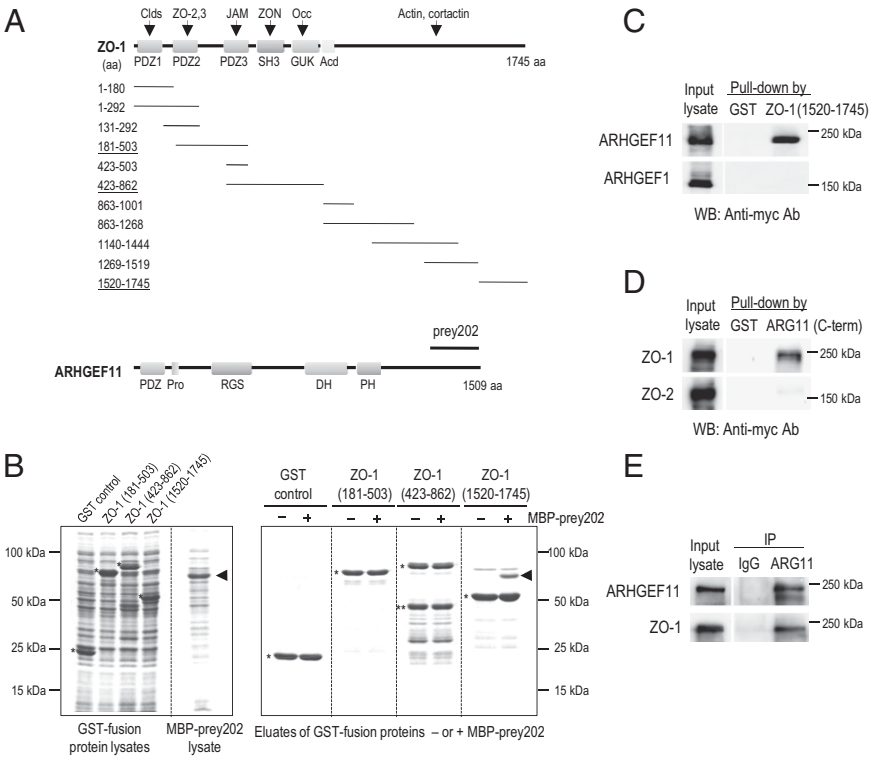

Fig. 1. Identification of ARHGEF11 as a ZO-1–binding protein. (*A*) Domain structure of ZO-1 and the fragments used to construct bait plasmids. Plasmids encoding the underlined fragments, aa 181 to 503, 423 to 862, and 1520 to 1745, were used to screen a mouse embryo cDNA prey library. The positive clone, prey202, contained a fragment encoding the C-terminal region of ARHGEF11, which possesses PDZ, RGS, DH, and PH domains. (*B*) In vitro binding assay between ARHGEF11 and ZO-1. The GST protein (control) or the GST fusion proteins encoding ZO-1 fragments aa 181 to 503, 423 to 862, or 1520 to 1745 (asterisks) bound to glutathione-Sepharose beads, was incubated with or without the lysate of *Escherichia coli*-expressing prey202 fused to the MBP (arrowhead). The eluates from beads incubated with a glutathione-containing buffer were separated by SDS/PAGE and analyzed by Coomassie brilliant blue staining. Two asterisks mark the degradation products of the native proteins. (*C* and *D*) Lysates of HeLa cells transfected with Myc-ARHGEF11 or Myc-ARHGEF1 were incubated with GST or GST-ZO-1(1520–1745) coupled with glutathione-Sepharose beads (*C*); lysates from Myc-ZO-1 or Myc-ZO-2 transfectants were incubated with GST or GST-ARG11 (C-term), which is the C-terminal region of ARHGEF11 corresponding to prey202 (*D*). Coprecipitated proteins were detected with anti-Myc antibodies. (*E*) Endogenous ARHGEF11 was immunoprecipitated from MCF7 cells, and the immunoprecipitants were analyzed by immunoblotting for ARHGEF11 and ZO-1. Mouse IgG was used as a control.

Next, we examined whether ARHGEF11 in cells interacted with ZO-1 (Fig. 1 *C* and *D*). An expression vector containing myc-tagged ARHGEF11 or ARHGEF1, another member of the RGS-RhoGEF family, was introduced into HeLa cells, and the cell lysates were incubated with GST or GST-ZO-1(1520–1745). Western blots of the eluted samples with an anti-myc antibody revealed significant amounts of ARHGEF11 in cells interacted with ZO-1(1520–1745), but no detectable interaction between ARHGEF1 and ZO-1(1520–1745) (Fig. 1*C*).

As a reverse experiment, we examined whether the C-terminal region of ARHGEF11 could pull down ZO-1 and the closely related ZO-2 in cells and found that ZO-1, but not ZO-2, was clearly precipitated by the C-terminal region of ARHGEF11 (Fig. 1*D*). Finally, the association between endogenous ARHGEF11 and ZO-1 was examined by immunoprecipitation. Endogenous ARHGEF11 was immunoprecipitated by using an anti-ARHGEF11 antibody from the lysates of MCF7 human mammary epithelial cells, and endogenous ZO-1 was found to be coprecipitated (Fig. 1*E*).

These findings strongly indicate that ARHGEF11, a member of the RGS-RhoGEF family proteins, specifically interacts with ZO-1 via ZO-1's C-terminal region, both in vitro and in vivo.

ARHGEF11 Localizes ZO-1–Dependently to TJs in Epithelial Cells and Tissues. ARHGEF11 has been shown to be a highly specific GEF for RhoA and to associate physically with the activated $G_{\alpha 12/13}$ proteins (14). However, its precise localization in epithelial cells and tissues is undetermined; in addition, molecular mechanisms regulating its cellular distribution pattern are not elucidated.

Thus, we first examined the localization of ARHGEF11 and ZO-1 in vivo by using frozen sections of the mouse mammary gland (Fig. 2*A*, *Middle*); in addition, the ARHGEF11 localization was compared with that of ERM (Ezrin/Radixin/Moesin), which is localized to the apical membrane domains (Fig. 2*A*, *Top*), and with that of E-cadherin that is distributed at the lateral membranes in addition to AJs (Fig. 2*A*, *Bottom*). In the mammary gland, the apical membrane domain faces the central lumen and is separated from the lateral membrane by ZO-1–positive TJs. We found that ARHGEF11 was clearly colocalized with ZO-1 at TJs, just beneath ERM and above E-cadherin labeling, respectively. Colocalization of ARHGEF11 and ZO-1 was also confirmed in other epithelial tissues, such as kidney (Fig. S1*A*), and in epithelial cell lines Caco-2, MCF7, and EpH4 (Fig. S1 *B* and *C*).

We previously established and analyzed mutant EpH4 cells depleted of ZO-1, ZO-2, or both ZO-1 and ZO-2 (12, 13, 15, 16). To investigate ARHGEF11 roles in relation to ZO-1 and ZO-2, we used EpH4 and its mutants. First, ARGEF11's localization and expression was examined in the ZO-1–KO EpH4 subline ZO1KO-EpH4. In the ZO1KO-EpH4 cells, ARHGEF11's localization at the TJs was significantly disturbed compared with the parental cells; most ARHGEF11 exhibited a cytoplasmic distribution with a punctate pattern (Fig. 2*B*, micrographs), whereas the level of ARHGEF11 was not altered by eliminating ZO-1 (Fig. 2*B*, Western blot). We also investigated whether the depletion of ZO-2 would affect the expression and/or localization of ARHGEF11 and found that ARHGEF11 was still targeted to the TJs in the ZO-2–depleted cells (Fig. S2). Therefore, ZO-1, but not the closely related ZO-2, is required to recruit ARHGEF11 to TJs.

Next, to examine whether ARHGEF11 is required for the proper intracellular localization of ZO-1, an ARHGEF11-specific siRNA or scrambled control siRNA was introduced into EpH4 cells (Fig. 2*C*). The effective knockdown of ARHGEF11 was confirmed by Western blot and immunofluorescence. We examined and quantified the ZO-1 expression level in ARHGEF11-depleted cells and control cells by using independently prepared lysates, and found that the ZO-1 expression was not significantly different between the two cell types. In addition, the targeting of ZO-1 to TJs appeared to be unaffected by ARHGEF11 depletion at 3 d after cell seeding (Fig. 2*C*).

Together, these data showed that ZO-1 specifically recruits ARHGEF11 to TJs in epithelial cells, but ZO-1 does not require ARHGEF11 for its own TJ targeting.

ARHGEF11 Depletion Delays Junction Assembly and Barrier Maturation. Although ARHGEF11 was apparently dispensable for targeting ZO-1 to TJs, its depletion might still have affected the formation

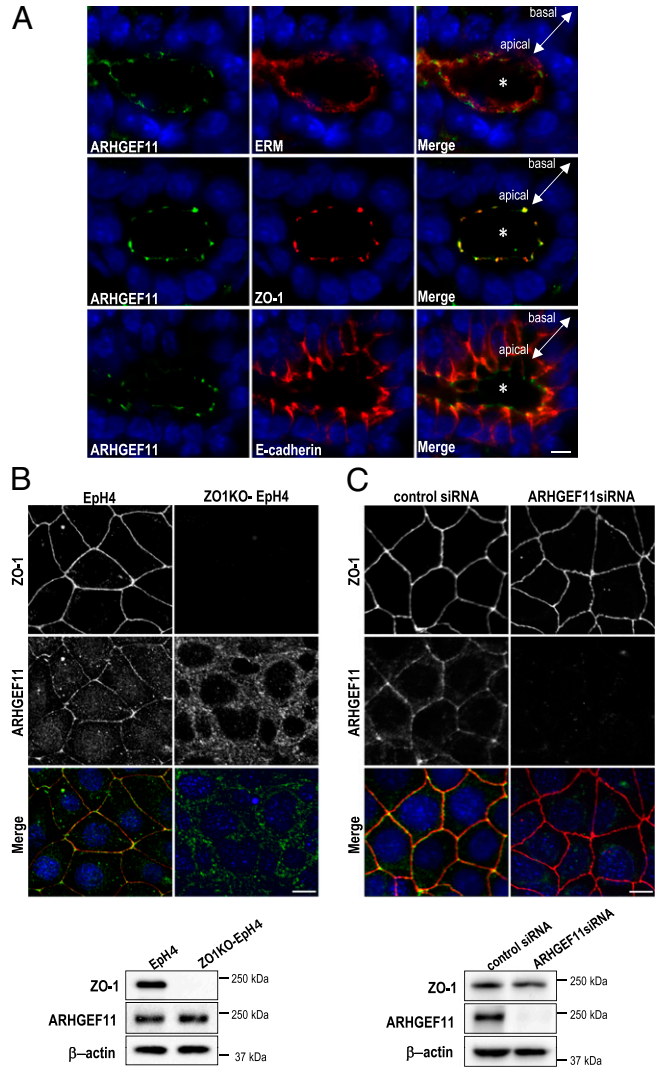

Fig. 2. ARHGEF11 localization to TJs is ZO-1–dependent. (*A*) Frozen sections of mouse mammary gland were coimmunostained for ARHGEF11 and ERM (*Top*), ARHGEF11 and ZO-1 (*Middle*), or ARHGEF11 and E-cadherin (*Bottom*). Asterisks indicate the lumen of the mammary ducts. (*B*) Expression and localization of ZO-1 and ARHGEF11 in EpH4 and ZO1KO-EpH4 cells was analyzed by immunoblotting and immunostaining. (*C*) Depletion of ARHGEF11 did not prevent ZO-1 from localizing to TJs. Control or ARHGEF11-specific siRNA was introduced into EpH4 cells, then the expression and localization of ZO-1 and ARHGEF11 were examined. Blue indicates DAPI staining. (Scale bars: 10 μm.)

and/or maintenance of cell–cell junctions and the paracellular barrier of epithelial cells. To address this issue, we used the calcium switch assay (Fig. 3). Confluent EpH4 cells transfected with control siRNA or ARHGEF11-specific siRNA were cultured in a low-Ca^{2+} medium (~2 μM Ca^{2+}) overnight, and the assembly of cell–cell junctions was initiated by switching the medium to one with a normal Ca^{2+} level (~1 mM Ca^{2+}). The degree of junction formation and maturation was evaluated by staining for myosin-IIB (Fig. 3 *A* and *B*) because it is reorganized during junction formation and found close to TJs in well-polarized epithelial cells as a major component of PJARs (17).

When calcium was depleted from the culture medium overnight, myosin-IIB labeling was observed throughout the cytoplasm, with poorly defined but increased intensity at the cell cortex in cells expressing either siRNA (Fig. 3*A*, 0 h). In the control siRNA EpH4 cells, ~3 h after the reintroduction of calcium, myosin-IIB labeling appeared as thick subcortical bundles that was gradually refined into a thin linear pattern at ~6 h. Finally, between 12 and 18 h, gaps between labeled regions were closed to build the complete PJAR architecture (Fig. 3*A*, control 12 h, 18 h).

In contrast, in the ARHGEF11-depleted cells, the junction assembly process was slower. Most myosin-IIB labeling remained in the thick bundle-like state even ~6 h after the switch to normal calcium, and the shift to linear labeling took much longer (~18 h). This attenuated phenotype was also detectable when the calcium switch assay was performed by using a coculture of control and ARHGEF11-depleted cells (Fig. 3*B*). In addition, we assessed the localization of JAM-A in cocultured cells (Fig. 3*C*). Approximately 6 h after the reintroduction of calcium, JAM-A exhibited dot-like pattern in the ARHGEF11-depleted cells, whereas it appeared as a dashed line in control cells (Fig. 3*C*, *Left*). Approximately 24 h after, JAM-A in control cells exhibited linear staining encircling cells that reflect TJ formation; on the contrary, JAM-A had an undulating appearance in the ARHGEF11-depleted cells (Fig. 3*C*, *Right*), suggesting that TJ formation was also attenuated by ARHGEF11 suppression.

To measure the functional integrity of the epithelial barrier in the ARHGEF11-depleted cells, we examined their transepithelial electrical resistance (TER). Confluent cells cultured on Transwell filters were subjected to calcium switch, and the barrier formation and maturation were assessed at 3, 6, 18, 24, and 36 h (Fig. 3*D*). The barrier function of the ARHGEF11-depleted cells was significantly attenuated compared with control cells, with a TER that was 30% to 40% of the control value at 36 h (Fig. 3*D*).

Although ZO-1 is highly concentrated at TJs in fully polarized epithelial cells, it is localized to a primordial spot-like AJ with cadherin–catenin complex at the initial phase of epithelial junction assembly (Fig. S3). Furthermore, a previous study implicated ZO-1 in the conversion from the spot-like AJ to the matured belt-like AJ, which is colocalized with PJARs (16). We assumed that the observed delay for junction assembly and barrier formation in the ARHGEF11-depleted cells might indicate the involvement of ARHGEF11 in the spot-like AJ, so ARHGEF11 distribution was examined. We also investigated p114RhoGEF, of which depletion was shown to cause the dissociation of ZO-1 from TJs and disruption of barrier in Caco-2 cells in a recent study (18), to dissect the function of these two RhoGEF proteins. We found that p114RhoGEF depletion seemed to not affect ZO-1 organization in EpH4 cells (Fig. S4); in addition, ARHGEF11, but not p114RhoGEF, colocalized with ZO-1 at the spot-like AJ (Fig. 3*E*, 1.5 h). Strikingly, an intense spot of fluorescent labeling was observed for both ARHGEF11 and ZO-1 in the low calcium culture condition (Fig. 3*E*, 0 h), suggesting that ARHGEF11 was constitutively associated with ZO-1. If so, ARHGEF11 could be quickly recruited to cell–cell adhesion sites to serve orchestrating the epithelial-type actomyosin architecture, and thus might be required at cell–cell contact sites from the initiation of the polarization process.

ARHGEF11 Depletion Affects MLC Activity and Association of E-Cadherin Complex with PJAR. To determine whether ARHGEF11 depletion affected actomyosin regulators that are downstream targets of Rho, we examined the activity of ERM, MLC, and Src by using phosphospecific antibodies by Western blotting ~6 h after the calcium switch (Fig. 4*A*). Although ERM and Src showed similar phosphorylation levels in control and ARHGEF11-depleted cells, p-MLC was significantly down-regulated (~50% reduction). Furthermore, by immunofluorescence, p-MLC signal appeared rather diffuse in the ARHGEF11-depleted cells, whereas the positive signal at cell–cell contact sites was clearly detected in cocultured control cells ~6 h after the calcium switch (Fig. 4*B*), a similar staining pattern to myosin-IIB at this stage (Fig. 3*A*, 6 h). We thought these observations indicated that the depletion of ARHGEF11 led to a reduction of the MLC activity at cell–cell adhesion sites that is required for PJAR formation.

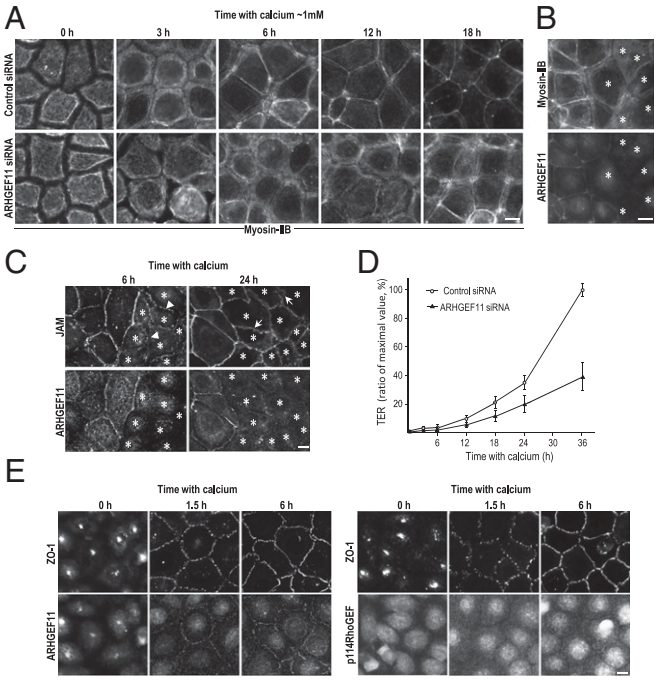

Fig. 3. ARHGEF11 is implicated in junction assembly and epithelial barrier formation. (*A*) EpH4 cells transfected with control or ARHGEF11-specific siRNA were cultured in low-calcium medium overnight. Junction assembly was initiated by reintroducing normal calcium medium. Cells were fixed at the indicated times and immunostained for myosin-IIB. (*B* and *C*) To further verify the effect of ARHGEF11 depletion on PJARs or TJs, a calcium switch assay was conducted using coculture of control and ARHGEF11-depleted cells. Cells were stained for myosin-IIB ~9 h after the calcium switch (*B*), and stained for JAM-A ~6 h or ~24 h after the calcium switch (*C*). Arrowheads and arrows indicate spot-like junctions and undulating appearance, respectively. Asterisks indicate ARHGEF11-depleted cells. (*D*) Establishment of the epithelial barrier was monitored by measuring the TER at the indicated times (data presented as means ± SD; $n = 3$). The *y* axis is the percentage of maximal TER measured in this experiment. (*E*) EpH4 cells were fixed at the indicated times after being returned to normal calcium, and the localization of ARHGEF11 or p114RhoGEF was compared with that of ZO-1. (Scale bars: 10 μm.)

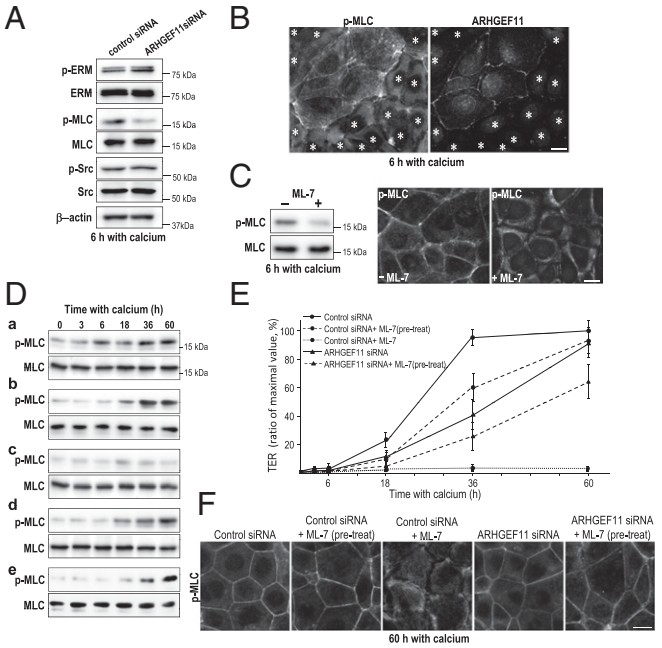

Fig. 4. ARHGEF11 depletion affects MLC activity. (*A*) Effect of ARHGEF11 depletion on the activity of actomyosin regulators. EpH4 cells transfected with control or ARHGEF11-specific siRNA were analyzed by Western blot by using antibodies to detect phospho-specific or total ERM, MLC, and Src ~6 h after the calcium switch. Representative data from three independent experiments are shown. (*B*) Coculture of control and ARHGEF11-depleted EpH4 cells were fixed ~6 h after the calcium switch and stained for p-MLC and ARHGEF11. Asterisks indicate ARHGEF11-depleted cells. (*C*) EpH4 cells were treated or not treated with ML-7 in a low calcium medium before the reintroducing normal calcium. The p-MLC was analyzed by Western blot and immunofluorescence after ~6 h culture in normal calcium medium. (*D*) The p-MLC level was examined by Western blotting over time in calcium switch. Calcium switch assay was conducted for control cells (*a*), control cells treated with 30 μM ML-7 in low calcium medium before calcium switch (pretreat) (*b*), control cells treated with 30 μM ML-7 before and after calcium switch (*c*), ARHGEF11 knockdown cells (*d*), and ARHGEF11 knockdown cells treated with 30 μM ML-7 in low-calcium medium before calcium switch (pretreat) (*e*). Cells were lysed at the indicated time and processed for Western blotting for detection of p-MLC level. Representative data from three independent experiments are shown. (*E*) TER was measured at the indicated times (data presented as means ± SD; $n = 3$). The *y* axis is the percentage of the maximal TER measured in this experiment. (*F*) Immunostaining for p-MLC in cells 60 h after calcium switch. (Scale bars: 10 μm.)

To clarify this possibility, we reduced MLC activity by ML-7, a specific inhibitor of MLC kinase, in calcium switch assays. The control cells were treated or not treated with ML-7 in low-calcium medium before the reintroduction of calcium, and the p-MLC was analyzed ~6 h after. We found the reduction of the p-MLC level by Western blot and the diffuse appearance of its labeling in cells treated with ML-7 (Fig. 4*C*). These phenotypes looked similar to those observed in ARHGEF11-depleted cells. The p-MLC level was also examined over time in calcium switch, and it showed elevation, especially approximately 6 h after, when myosin began to organize into thin linear pattern, and then it seemed to reach a steady state (Fig. 4*D*, *a*). The cells treated with ML-7 showed retardation in increase of p-MLC level, but it became comparable to that in nontreated cells (Fig. 4*D*, *b*), and the p-MLC localization pattern was almost same between ML-7–treated and untreated cells at 60 h (Fig. 4*F*). In contrast, when cells were treated with ML-7 before and after the calcium switch, the increase of p-MLC level and rearrangement of its distribution was not observed even 60 h later (Fig. 4 *D*, *c*, and *F*). We also measured TER over time and found that the elevation of TER was significantly delayed or abolished when cells were treated with ML-7 before or before and after the calcium switch, respectively (Fig. 4*E*). Although alteration pattern of p-MLC level and TER over time was not exactly the same, ML-7 had similar effects on both properties and p-MLC organization. When ARHGEF11-depleted cells were treated with ML-7 before the reintroduction of calcium, p-MLC level exhibited further reduction at time 0 and delayed in its increase (Fig. 4*D*, *e*) compared with that in nontreated ARHGEF11-depleted cells (Fig. 4*D*, *d*). Likewise, TER elevation was retarded and p-MLC rearrangement was slightly altered at ~60 h (Fig. 4 *E* and *F*). These results suggest that the activation of MLC is required for junction assembly and barrier maturation, and ARHGEF11 as well as other sources are involved in MLC activation for junction regulation.

Next, to elucidate the effect of ARHGEF11's depletion on junction maintenance, the organization of TJs, AJs, and PJARs was analyzed in coculture of EpH4 cells transfected with control or ARHGEF11 siRNA and maintained for ~3 d under confluent conditions (Fig. S5*A*). Immunostaining for occludin revealed that signal intensity and localization pattern were almost the same between control and ARHGEF11-depleted cells, and the organization of myosin-IIB in PJARs did not seem disturbed in the ARHGEF11-depleted cells. In contrast, the lateral distribution of E-cadherin appeared to be increased. When cells were treated with a buffer containing 0.5% CHAPS, E-cadherin and β-catenin in the

ARHGEF11-depleted cells showed increased solubility, whereas neither the TJ nor PJAR components exhibited obvious differences (Fig. S5*B*). Therefore, ARHGEF11 depletion appeared to affect the association between the E-cadherin complexes and PJARs, but the overall organization of established TJs, AJs, and PJARs was not appreciably affected.

ARHGEF11 Is Critical for PJAR Remodeling by ZO-1. When ZO-1 and ZO-2 are depleted simultaneously, the formation of TJ strands and establishment of barrier are severely impaired (12). In addition, the PJAR components are not organized properly under these depletion conditions (13). As the expression of either ZO-1 or ZO-2 is sufficient to prevent such defects, these proteins are believed to play redundant and critical roles in organizing the TJ and PJAR architecture (12, 13).

To determine whether ARHGEF11 is involved in the ZO-mediated regulation of PJARs and TJs organization, we used an EpH4 subline, ZO1KO·ZO2KD-EpH4, in which ZO-1 was knocked out and ZO-2 was depleted by using an shRNA (12). ZO-1 expression vector was introduced into ZO1KO·ZO2KD-EpH4 cells with the control or ARHGEF11-targeted siRNA (Fig. 5*A*), and the cells were analyzed 3 d after replating. The reexpressed ZO-1 was clearly localized to cell–cell junctions in both transfectants (Fig. 5*B*, *Top Left* and *Middle*), and the PJARs, represented by myosin-IIB, were properly remodeled at the ZO-1–positive cell–cell adhesion sites in ZO1KO·ZO2KD-EpH4 cells cotransfected with control siRNA (Fig. 5*B*, *Left*). However, in the ARHGEF11-depleted ZO1KO·ZO2KD-EpH4 cells, the PJARs were not rescued by ZO-1 (Fig. 5 *B*, *Middle*, and *C*).

To dissect whether the ARHGEF11-binding domain was necessary for ZO-1 to remodel an immature PJAR, we introduced ZO-1ΔCT, a mutant ZO-1 lacking the ARHGEF11-binding C-terminal domain, into the ZO1KO·ZO2KD-EpH4 cells. Although ZO-1ΔCT was localized to cell–cell contact sites just like WT ZO-1, myosin-IIB remained as diffuse bundles, indicating that the PJARs were not established properly (Fig. 5 *B*, *Right*, and *C*). To clarify whether endogenous ARHGEF11 was recruited to the TJs in these cells, ZO1KO·ZO2KD-EpH4 cells transfected with WT ZO-1 or ZO-1ΔCT were processed for immunostaining. Endogenous ARHGEF11 was clearly detected at TJs in cells expressing WT ZO-1 (Fig. 5*D*, *Upper*, arrows); however, ARHGEF11 remained cytoplasmic when ZO-1ΔCT was expressed, even though the ZO-1ΔCT was localized at cell–cell junctions (Fig. 5*D*, *Lower*, arrowheads). We also investigated the exogenous ARHGEF11 in ZO1KO·ZO2KD-EpH4 cells (Fig. S6). Although almost no Myc-ARHGEF11 was located at cell–cell junctions in ZO1KO·ZO2KD-EpH4 cells, it was efficiently concentrated at TJs when cotransfected with WT ZO-1. On the contrary, Myc-ARHGEF11ΔCT, which lacked the C-terminal ZO-1–binding domain, was distributed in the cytoplasm, even in the presence of WT ZO-1, implying that the C-terminal domain of ARHGEF11 is necessary for its targeting to TJs via ZO-1.

Finally, we addressed whether the ZO-1/ARHGEF11 complex and ZO-2 regulate the organization of PAJRs and TJs through independent molecular pathways. To this end, we used ZO2KD-EpH4 cells, which did not show significant defects in TJs and PJARs (12). When we depleted both ARHGEF11 and ZO-2 by introducing ARHGEF11 siRNA into ZO2KD-EpH4 cells, myosin-IIB and occludin were aberrantly localized (Fig. 5*E*, asterisks), which is similar to the phenotype that is observed when both ZO-1 and ZO-2 are suppressed (12, 13).

Together, our data indicate that ARHGEF11, a member of the RGS-RhoGEF family, specifically cooperates with ZO-1, and their direct interaction via their C-terminal regions is crucial for the proper establishment of PJARs and TJs in epithelial cells.

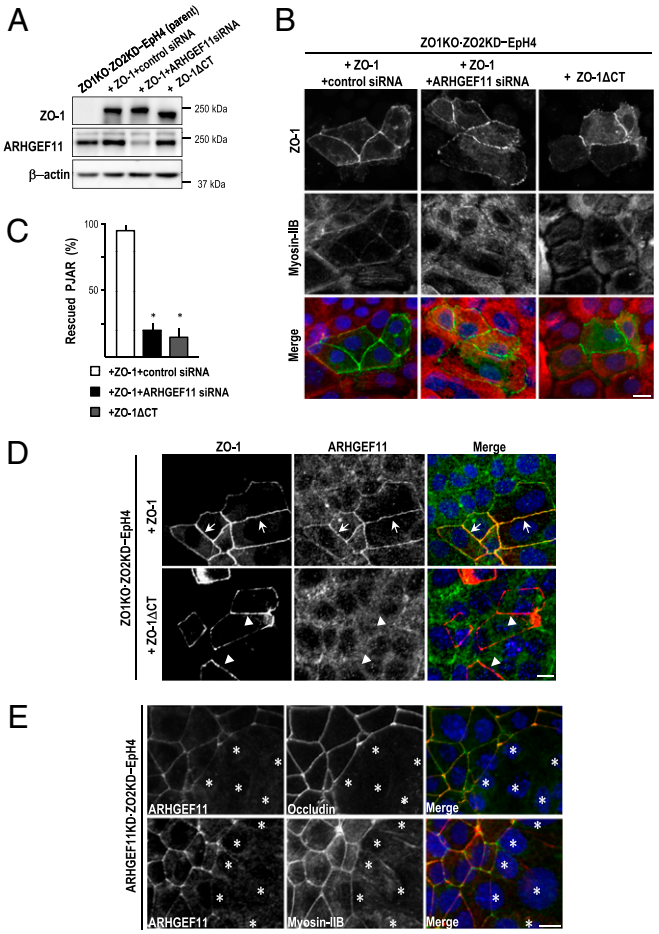

Fig. 5. ARHGEF11 plays a crucial role in the ZO-1–mediated remodeling of PJARs. (*A*–*C*) EpH4 cells depleted of ZO-1 and ZO-2 (ZO1KO·ZO2KD-EpH4) were cotransfected with a ZO-1 expression vector and control or ARHGEF11-specific siRNA, or transfected with ZO-1ΔCT (lacking aa 1520–1745). The expression of ZO-1 and ARHGEF11 was examined by Western blotting (*A*). (*B*) Distribution of the reexpressed WT or mutant ZO-1 was compared with that of myosin-IIB. (*C*) The number of cells exhibited the formation of PJAR represented by organized myosin-IIB as a thin line encircling cells was divided by the number of cells that were positive for reexpressed ZO-1. The percentage of the value was defined as rescued PJARs (*y* axis; data presented as mean ± SD; $n = 3$; $^*P < 0.001$). (*D*) Recruitment of ARHGEF11 to TJs by WT or mutant ZO-1 was examined. ZO1KO·ZO2KD-EpH4 cells transfected with WT or ΔCT mutant ZO-1 were immunostained for ZO-1 and ARHGEF11. Arrows and arrowheads indicate cell–cell adhesion sites. (*E*) Effect of the simultaneous depletion of ARHGEF11 and ZO-2 on junction formation. ARHGEF11-specific siRNA was introduced into ZO2KD-EpH4 cells. The cells were stained for ARHGEF11 with myosin-IIB or occludin to investigate the organization of PJARs or TJs, respectively. Asterisks indicate ARHGEF11-depleted cells. The cells were analyzed 3 d after replating (*A*–*E*). (Scale bars: 10 μm.)

Discussion

Here, we identified ARHGEF11 as a regulator for ZO-1–dependent junction assembly and barrier formation in epithelial cells. Previous studies showed that ZO-1 and the RhoA pathway regulates the organization of TJs and PJARs, the barrier function in epithelial cells, and the maturation of AJs during epithelial cell polarization (9, 10, 12, 13, 16). However, the direct molecular evidence connecting ZO-1 with the RhoA pathway has not been determined.

The present study shows that a GEF protein for RhoA, ARHGEF11, directly and specifically associates with ZO-1 (Fig. 1). ZO-1 recruited ARHGEF11 to TJs in polarized epithelial cells (Fig. 2) and to the primordial spot-like AJ (Fig. 3). This

CELL BIOLOGY

interaction in cells possibly enables the spatially restricted activation of RhoA and MLC at cell–cell adhesion sites, promoting contraction of the junction-associated actomyosin cytoskeleton, which induces the assembly of junctions and the consequent formation of the epithelial barrier.

We previously demonstrated that TJs and the epithelial barrier are severely compromised when both ZO-1 and ZO-2 are depleted, but the depletion of ZO-1 alone retards junction assembly and barrier establishment (14, 15). Here, we found that depletion of ARHGEF11 or the inhibition of its association with ZO-1 caused similar defects (Fig. 5). As ZO-2 did not interact with the C-terminal region of ARHGEF11 (Fig. 1*D*), we postulate that the ZO-1/ARHGEF11 complex and ZO-2 regulate the PJAR and TJ organization through independent molecular pathways. The results that cells depleted of both ARHGEF11 and ZO-2 exhibited similar defects to cells depleted of ZO-1 and ZO-2 support this presumption. Recently, the depletion of p114RhoGEF alone was reported to be sufficient to cause the dissociation of ZO-1 from TJs and disruption of barrier in Caco-2 via modulating MLC (18); however, such defects were not observed in our experiments with EpH4 (Fig. S4). It is possible that molecular machinery regulating epithelial junctions could vary among different cell types; in addition, our data with ML-7 suggest the existence of additional sources other than ARHGEF11 in MLC-dependent junction regulation. The existence of a redundant pathway to maintain integrity of epithelial cells seems very likely, because disruption of the epithelial barrier can rapidly become life-threatening.

An earlier study showed that the constitutive activation of MLC kinase induced increased TJ permeability (10), which seems to be contradictory to our results. On the contrary, the inhibition of Rho kinase, which is upstream of MLC, was shown to prevent the formation of TJ and barrier in calcium switch assays (19); similar effects were observed in EpH4 cells treated with ML-7 (Fig. 4). We assume that the appropriate contraction force of actomyosin at the cell–cell contact sites is necessary, and that an excessive or a reduced p-MLC level could lead to inadequate actomyosin contraction, and consequently to the impaired formation and function of TJs and PJARs. Considering this point, opposing signals that prevent excess constriction induced by the activation of RhoA and MLC would be crucial to maintain the integrity of epithelial cells. One study indicated that the activation of Rac antagonizes Rho-mediated actomyosin contraction and contributes to maintain appropriate permeability (20). In another recent study, aPKC was shown to inhibit excess actomyosin contraction and allow cells to retain normally shaped apical domains (21). Determining if these pathways have a molecular linkage to the ZO-1/ARHGEF11 pathway, and further, elucidating unidentified pathways that ensure the balance of PJAR constriction, will permit the dissection of the precise molecular mechanisms that regulate the organization of junctions and the junction-associated cytoskeleton.

ARHGEF11 contains an RGS domain, which regulates the activity of $G\alpha_{12/13}$ proteins; thus, it provides a direct link from G protein-coupled signaling to RhoA. Interestingly, it was reported that $G\alpha_{12}$ is localized to TJs and interacts directly with ZO-1 (22). The treatment of endothelial cells with lysophosphatidic acid, a stimulator of $G\alpha_{12/13}$, was shown to modulate PJAR assembly (23), and a recent study reported that ARHGEF11 is one of the five SNPs identified as genetic susceptibility loci for intracranial aneurysm, which has defects in the brain blood vessels, suggesting that ARHGEF11 is also involved in endothelial regulations (24). It might be possible that ZO-1 and G protein-coupled stimulation, respectively, define the spatial and temporal activation of a specific RhoGEF that regulates the epithelial and endothelial junctions and barrier.

In conclusion, the present findings contribute a key element toward understanding the control of the assembly and maturation of cell–cell junctions and barrier formation in epithelial cells. This information will be of help to lead a better understanding of how epithelial cells and cell sheets are integrated to maintain homeostasis in multicellular organisms.

Materials and Methods

The transfection of DNA and siRNA was performed according to the manufacturer's instruction. The details of all the experimental procedures are described in the *SI Text*. The antibodies and other reagents are also described in the *SI Text*.

ACKNOWLEDGMENTS. This work was supported by a Grant-in-Aid for Scientific Research from the Ministry of Education, Culture, Sports, Science, and Technology of Japan (to M.I.).

1. Nelson WJ (2003) Adaptation of core mechanisms to generate cell polarity. *Nature* 422:766–774.
2. Bryant DM, Mostov KE (2008) From cells to organs: Building polarized tissue. *Nat Rev Mol Cell Biol* 9:887–901.
3. Hartsock A, Nelson WJ (2008) Adherens and tight junctions: Structure, function and connections to the actin cytoskeleton. *Biochim Biophys Acta* 1778:660–669.
4. Tsukita S, Furuse M, Itoh M (2001) Multifunctional strands in tight junctions. *Nat Rev Mol Cell Biol* 2:285–293.
5. Itoh M, et al. (2001) Junctional adhesion molecule (JAM) binds to PAR-3: A possible mechanism for the recruitment of PAR-3 to tight junctions. *J Cell Biol* 154:491–497.
6. Itoh M, Nagafuchi A, Moroi S, Tsukita S (1997) Involvement of ZO-1 in cadherin-based cell adhesion through its direct binding to alpha catenin and actin filaments. *J Cell Biol* 138:181–192.
7. Yu D, et al. (2010) MLCK-dependent exchange and actin binding region-dependent anchoring of ZO-1 regulate tight junction barrier function. *Proc Natl Acad Sci USA* 107:8237–8241.
8. Nusrat A, et al. (1995) Rho protein regulates tight junctions and perijunctional actin organization in polarized epithelia. *Proc Natl Acad Sci USA* 92:10629–10633.
9. Jou TS, Schneeberger EE, Nelson WJ (1998) Structural and functional regulation of tight junctions by RhoA and Rac1 small GTPases. *J Cell Biol* 142:101–115.
10. Shen L, et al. (2006) Myosin light chain phosphorylation regulates barrier function by remodeling tight junction structure. *J Cell Sci* 119:2095–2106.
11. Wallace SW, Magalhaes A, Hall A (2011) The Rho target PRK2 regulates apical junction formation in human bronchial epithelial cells. *Mol Cell Biol* 31:81–91.
12. Umeda K, et al. (2006) ZO-1 and ZO-2 independently determine where claudins are polymerized in tight-junction strand formation. *Cell* 126:741–754.
13. Yamazaki Y, et al. (2008) ZO-1- and ZO-2-dependent integration of myosin-2 to epithelial zonula adherens. *Mol Biol Cell* 19:3801–3811.
14. Siehler S (2009) Regulation of RhoGEF proteins by G12/13-coupled receptors. *Br J Pharmacol* 158:41–49.
15. Umeda K, et al. (2004) Establishment and characterization of cultured epithelial cells lacking expression of ZO-1. *J Biol Chem* 279:44785–44794.
16. Ikenouchi J, Umeda K, Tsukita S, Furuse M, Tsukita S (2007) Requirement of ZO-1 for the formation of belt-like adherens junctions during epithelial cell polarization. *J Cell Biol* 176:779–786.
17. Smutny M, et al. (2010) Myosin II isoforms identify distinct functional modules that support integrity of the epithelial zonula adherens. *Nat Cell Biol* 12:696–702.
18. Terry SJ, et al. (2011) Spatially restricted activation of RhoA signalling at epithelial junctions by p114RhoGEF drives junction formation and morphogenesis. *Nat Cell Biol* 13:159–166.
19. Walsh SV, et al. (2001) Rho kinase regulates tight junction function and is necessary for tight junction assembly in polarized intestinal epithelia. *Gastroenterology* 121: 566–579.
20. Wojciak-Stothard B, Tsang LY, Haworth SG (2005) Rac and Rho play opposing roles in the regulation of hypoxia/reoxygenation-induced permeability changes in pulmonary artery endothelial cells. *Am J Physiol Lung Cell Mol Physiol* 288:L749–L760.
21. Ishiuchi T, Takeichi M (2011) Willin and Par3 cooperatively regulate epithelial apical constriction through aPKC-mediated ROCK phosphorylation. *Nat Cell Biol* 13:860–866.
22. Meyer TN, Schwesinger C, Denker BM (2002) Zonula occludens-1 is a scaffolding protein for signaling molecules. Galpha(12) directly binds to the Src homology 3 domain and regulates paracellular permeability in epithelial cells. *J Biol Chem* 277: 24855–24858.
23. van Nieuw Amerongen GP, Vermeer MA, van Hinsbergh VW (2000) Role of RhoA and Rho kinase in lysophosphatidic acid-induced endothelial barrier dysfunction. *Arterioscler Thromb Vasc Biol* 20:E127–E133.
24. Akiyama K, et al. (2010) Genome-wide association study to identify genetic variants present in Japanese patients harboring intracranial aneurysms. *J Hum Genet* 55: 656–661.